Available online at www.eccomasproceedia.org
Eccomas Proceedia COMPDYN (2023) 3754-3769

ECCOMAS
Proceedia

COMPDYN 2023
9th ECCOMAS Thematic Conference on
Computational Methods in Structural Dynamics and Earthquake Engineering
M. Papadrakakis, M. Fragiadakis (eds.)
Athens, Greece, 12-14 June 2023

THE EFFECT OF GROUND MOTION INCIDENCE ANGLE FOR SCOURED HIGHWAY BRIDGES

S. Ateş[1] and Ö. Avşar[2]

[1] Department of Civil Engineering, Eskisehir Technical University
Iki Eylul Kampusu, 26555 Eskisehir, Turkey
e-mail: serenayates@ogr.eskisehir.edu.tr

[2] Department of Civil Engineering, Eskisehir Technical University
Iki Eylul Kampusu, 26555 Eskisehir, Turkey
e-mail: ozguravsar@eskisehir.edu.tr

Abstract

Bridges are usually built to connect two pieces of land where water flows between them. Over time, for the water crossing bridges it is inevitable to occur scour around bridge substructure and this may affect both the seismic demands and capacity of bridge members. Besides, the ground motion incidence angle is another critical issue that can amplify the seismic demands imposed on the bridges. In this study, it is aimed to investigate the seismic performance of a highway bridge which has a uniform scour around its piles. A soil structure interacted reinforced concrete bridge consisting of prestressed I-sectioned beams and deck is modeled in OpenSees program. Scour depth is varied from 0 m (no scour) to 5 m depth with a uniform increment of 1 m. During nonlinear time history analysis, 7 different strong ground motion records with their 3 components are used. To obtain critical incidence angle, horizontal components of ground motions are rotated from 0° to 180° with an increment of 15° by using linear transformation equations. Superstructure displacement, pier curvature and shear force demands are investigated for each scour depth and earthquake incidence angle in the scope of the study. Both scour depth and earthquake incidence angle affect the seismic response of the investigated highway bridge under the selected ground motion records.

Keywords: Scour, Incidence angle, Reinforced concrete bridge, Nonlinear time history analysis.

ISSN:2623-3347
Peer-review under responsibility of the organizing committee of COMPDYN 2023.
doi: 10.7712/120123.10677.20995

1 INTRODUCTION

Bridges are particularly expensive and vital type of construction since they are the backbone of community life and one of the most crucial parts of the road network. In the event of an earthquake, the existing bridges should be serviceable to provide connection for the emergency and rescue teams to the affected area and to maintain the sustainability of social life. Even if bridge-like structures are constructed in compliance with the regulations, they are still susceptible to damage from many external factors including aging, natural disasters etc. In such circumstances, it is crucial for designers to calculate the actual demands that will be imposed on the structural members in order to predict potential structural damage. As a result, in recent years, researchers have examined the demands that occur in bridges under various effects [1, 2, 3]. Scour, which is an important phenomenon, is caused by water erosion as it flows and it becomes a stunning occurrence for bridges built in flood region areas. According to U.S. Department of Transportation [4], 3 types of scour can exist in a flood region area; long term aggradation and degradation of the river bed, contraction scour at the bridge and local scour at the piers or abutments. The most important one is the local scour for bridge type structures because it occurs around the substructure of bridge and it may affect the seismic demand of members during earthquake or any other natural hazards. Moreover, unexpected damage to bridges may occur when the combined effects of scour and earthquake occur [5, 6, 7]. Nonlinear time history analysis is frequently used to calculate the seismic demands of bridge elements during an earthquake. Real or artificial ground motion suits are employed for the simulations. Although the horizontal ground motion components are frequently applied on the global axes of the structure, the incidence angle at which the horizontal ground motion components affecting the structure is generally different from the global axis. Numerous investigations have found that when the earthquake incidence angle is taken into account, the seismic demands of elements are affected considerably [8, 9, 10, 11, 12].

In this study, it is aimed to determine the effect of ground motion incidence angle in nonlinear analysis for scoured highway bridges. A soil structure interacted concrete bridge model with prestressed I beams, and a single column bent was modelled in the OpenSees platform. It has 4 spans with 35 m span length and 12 m width and total length of the bridge is 140 m. Scour depth was changed starting from 0 m (no Scour) to 5 m with a uniform increment of 1m for each piles. According to the Principles for the Design of Highway and Railroad Bridges and Viaducts Under the Impact of Earthquakes [13], nonlinear time history analyses should be conducted under 7 strong ground motion records. The incidence angle of the ground motion pairs was rotated starting from 0° to 180° with an increment of 15° by using linear transformation equations. Deck displacement in longitudinal and transverse direction, shear and curvature demand for bridge piers are the seismic demand parameters for investigating the effectiveness of the method. It is thought that this study will contribute to the evaluation of the seismic demands more realistically that arise under multiple effects, such as earthquake and scour, in the elements of a typical bridges.

2 CHARACTERISTICS AND ANALYTICAL MODELING OF BRIDGES

2.1 Bridge properties

The bridge used in the study is a reinforced concrete highway bridge consisting of prestressed I-section beams and continuous deck and it is found mostly in Turkey. The bridge superstructure has 4 spans as seen in Figure 1, each span has 35 m length and 12 m width and the total length of the bridge is 140 m. The superstructure consists of 8 prestressed beams and a continuous reinforced concrete deck. Deck thickness is 22 cm. Concrete grade is C40 for the

prestressed beams, C25 for other elements, and reinforcing steel grade is S420. The bridge substructure consists of a cap beam, single column piers and abutments. Each of the column piers is H=8.7 m high and consists of an oval section of B_c=1.2 m and D=4 m. Both the piers and abutments are supported on the pile cap. The cap beam has a rectangular section with a width of 1.2 m and a depth of 1.75 m. There are 450x250x40 mm elastomeric bearings under each prestressed beam. Moreover, pile cap has a rectangular section with dimensions B_{cap}=2.5m, L_{cap}=5m and a height of H_{cap}=1.5m. Under this pile cap, there are 6 circular piles with a diameter of D_{pile}=1m and a height of H_{pile}=20m. Concrete grade is also taken as C25 and steel grade is S420 for pile elements.

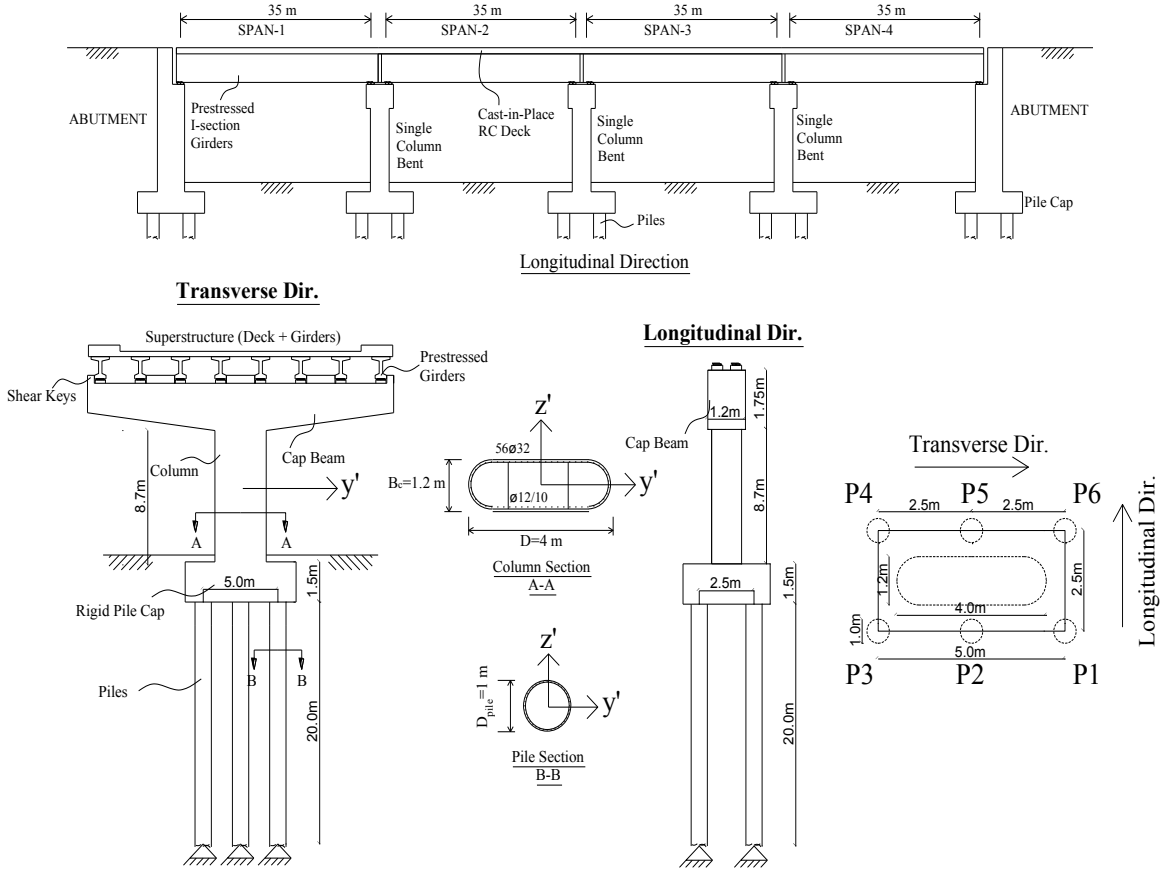

Figure 1: Properties of bridge members.

2.2 Analytical modeling

The 3 dimensional analytical model of the reinforced concrete highway bridge used in the study was created using the frame elements in the OpenSees program as seen in Figure 2. Because of the elastomeric bearings between superstructure and substructure, superstructure members such as deck and girders were modelled by using elastic beam column elements and masses are distributed at equally spaced nodes. Fiber section elements were used to create bent columns in order to simulate the nonlinear behavior. Abutment-deck pounding and deck-shear key pounding were defined using nonlinear pounding elements in both the longitudinal and transverse directions, respectively. They have 5 cm gap in longitudinal and 2.5 cm gap in transverse direction. In addition, springs were used at the abutments to simulate the soil - structure interaction with regard to Caltrans [14]. While defining the pile cap, rigid elastic beam column elements were used in OpenSees. Column pier and piles were connected to the

pile cap with also rigid elements. Piles were assumed to be in the elastic limits during earthquake therefore, they were defined by using elastic beam column elements in the model.

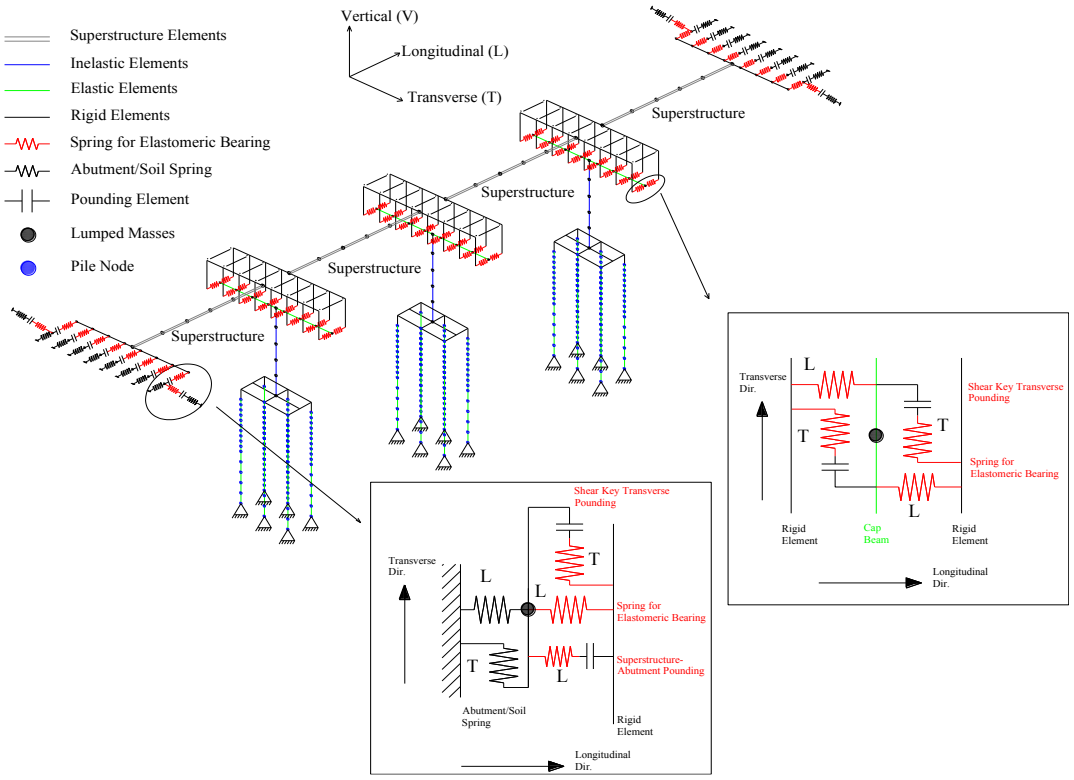

Figure 2: Analytical bridge model constructed in OpenSees.

2.3 Soil-structure interaction

The foundation of the piles is affected by axial and lateral loads caused by the surrounding soil, particularly during earthquakes. In order to achieve realistic results, it is essential to take soil structure interaction into account while modeling the structural system for bridges. In the literature, many of the researchers used soil springs to reflect this interaction [2, 5, 15, 16] During the modeling process in the OpenSees program, "Py Simple1" material model was used for lateral soil resistance and "Tz Simple1" material model was used for axial resistance. The pile elements were divided into 0.5 m long members for the first 10 m length below the pile cap and 1 m long members for the last 10 m. The springs were assigned to the nodes of these small elements. P-y springs were defined in the horizontal direction (both longitudinal and transverse directions) of the bridge and t-z springs were assigned in the vertical direction as seen in Figure 3.

The soil around the piles was chosen as sand with a unit weight γ_{sand}=18 kN/m^3 and angle of internal friction Ø=25°. Uniaxial material properties of p-y springs were calculated according to the American Petroleum Institute (API) [17]. The relationship between lateral soil resistance (P) and deflection (y) can be calculated by using Equation (1);

$$P = A \cdot P_u \cdot tanh\left[\frac{k \cdot H}{A \cdot P_u} \cdot y\right] \quad (1)$$

where, A=factor to account for cyclic or static loading condition and evaluated by A=0.9 for cyclic loading. P_u (kN/m) is the ultimate bearing capacity at depth H (m), k is the initial modulus of subgrade reaction, given in API [17] as function of internal friction Ø. H (m) is the depth from ground level and y (m) is the lateral deflection. The ultimate lateral capacity for sand can be calculated by using Equation (2) and (3) for shallow and deep depths, respectively. At a given depth the smallest value of the given equation should be used as P_u.

$$P_{us} = (C_1 \cdot H + C_2 \cdot D) \cdot \gamma \cdot H \tag{2}$$

$$P_{ud} = C_3 \cdot D \cdot \gamma \cdot H \tag{3}$$

In these equations, P_u is the ultimate resistance (kN/m) for s=shallow and d=deep. γ is the effective soil weight (kN/m3), H is depth (m), C_1, C_2 and C_3 are the coefficients determined from API [17] as function of Ø and D is the average pile diameter from surface to depth (m).

The uniaxial material properties of t-z spring was calculated for sand type soil [18]. Ultimate axial soil resistance was calculated by using Equation (4);

$$T_{ult1} = K_0 \cdot \gamma \cdot H \cdot P_{Perimeter} \cdot tan\delta \tag{4}$$

$$T_{ult} = T_{ult1} \cdot L \tag{5}$$

$$Z_{50} = \frac{t_{ult}}{K_f} \tag{6}$$

where, T_{ult1} is the ultimate axial bearing capacity of pile with a unit of kN/m. K_0 is the coefficient of the lateral earth pressure at rest, taken as K_0=0.4, H is the depth (m), P is the perimeter of pile surface and δ is interface friction between soil and pile, take as δ=0.8xØ to be representative of a smooth precast concrete pile [18]. After calculating T_{ult1}, it should be converted to the force unit (T_{ult}) by multiplying length of the pile section as given in Equation (5). Z_{50} represents displacement at 50% of T_{ult}. It can be calculated by using Equation (6) and K_f is initial modulus of side resistance [19].

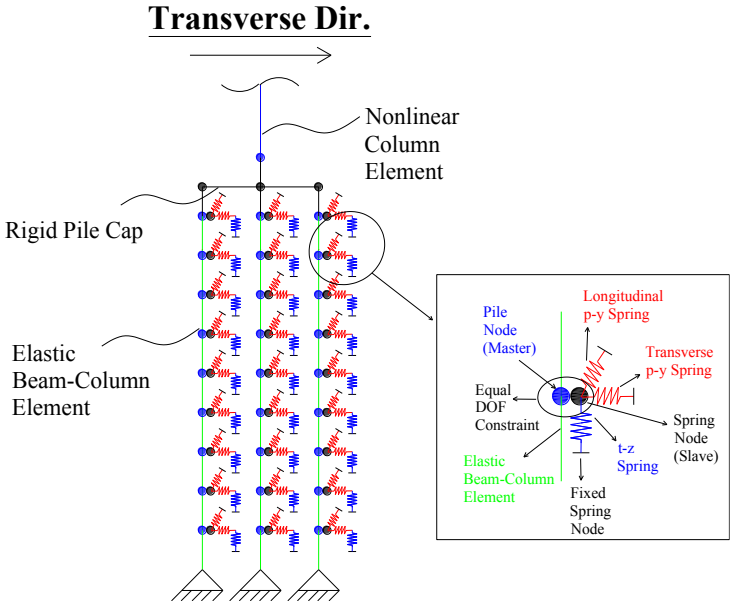

Figure 3: Description of nonlinear p-y and t-z springs on the bridge piles.

2.4 Scour Effect

Scour is a significant phenomenon that, as previously mentioned, may have an impact on the seismic demands for bridge members. In this study, it is aimed to determine seismic demands of scoured bridge members under the effect of strong ground motions. Therefore 6 different scour cases were created in the OpenSees program. The depth of scour around bridge piles was changed starting from 0 m (no scour) to 5 m with an increment of 1 m as seen in Figure 4. For each scour depth, nonlinear springs were removed from the pile nodes and soil properties were recalculated for each depth.

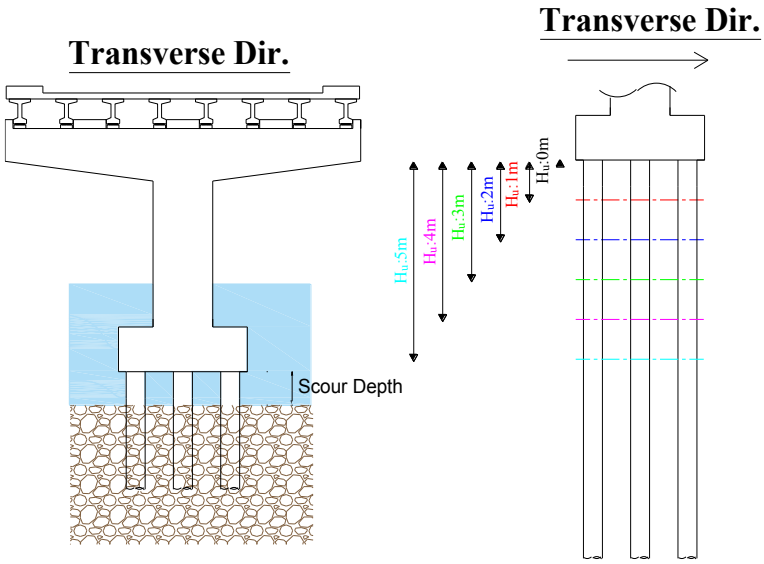

Figure 4: The change of uniform scour depth (Hu).

3 GROUND MOTION PROPERTIES

3.1 Selection and scaling of ground motion records

Nonlinear time history analysis of the bridge analytical model created within the scope of the study were performed using the OpenSees program. By using Pacific Earthquake Engineering Research Center [20] database, 7 strong ground motion suits selected and scaled according to Principles for the Design of Highway and Railroad Bridges and Viaducts Under the Impact of Earthquakes [13]. The properties of the horizontal components of selected ground motions are given in Table 1. Assuming that the bridge used in the study is located in Eskisehir, a location was chosen by using the Turkey Earthquake Hazard Map [21] web interface. Spectral acceleration-period graph was obtained for the ZD soil class and DD-2 (earthquake ground motion level with 10% probability of exceedance in 50 years) level of this location. The amplitudes of the selected earthquake ground motion components are scaled according to the rule given in section 2.5.2.2. in the regulations that the ratio of the average amplitudes of the resultant spectra of all selected records between the 0.2 T_p and 1.5 T_p period range to the amplitudes of the design acceleration spectrum in the same period range is not less than 1.3 as given in Figure 5, where T_p is the fundamental period of the bridge. The specified scale factor should be considered for both perpendicular horizontal components and vertical component of the ground motion records.

No	Event	Station	Mw	Fault Type	Component	PGA (g)	PGV (cm/s)	PGD (cm)	Scale Factor
1	Coyote Lake, 1979	Gilroy Array #6	5.74	Strike slip	230° 320°	0.42 0.31	44.34 25.39	12.44 4.38	1.0
2	Morgan Hill, 1984	Anderson Dam	6.19	Strike slip	250° 340°	0.42 0.28	25.40 27.80	4.43 6.43	1.0
3	Imperial Valley, 1979	El Centro Array #4	6.53	Strike slip	140° 230°	0.48 0.37	39.64 80.41	25.13 74.26	1.0
4	Landers, 1992	Lucerna	7.28	Strike slip	260° 345°	0.72 0.78	133.40 28.10	113.92 25.53	1.0
5	Düzce, 1999	Duzce	7.14	Strike slip	180° 270°	0.40 0.51	71.15 84.23	49.69 48.03	1.0
6	Superstition Hills, 1987	El Centro Imp. Co. Cent	6.54	Strike slip	0° 90°	0.35 0.25	48.07 41.79	19.27 21.85	1.0
7	Kocaeli, 1999	İzmit	7.51	Strike slip	90° 180°	0.23 0.16	38.29 22.33	24.29 11.84	1.0

Table 1: Properties of the selected ground motion records

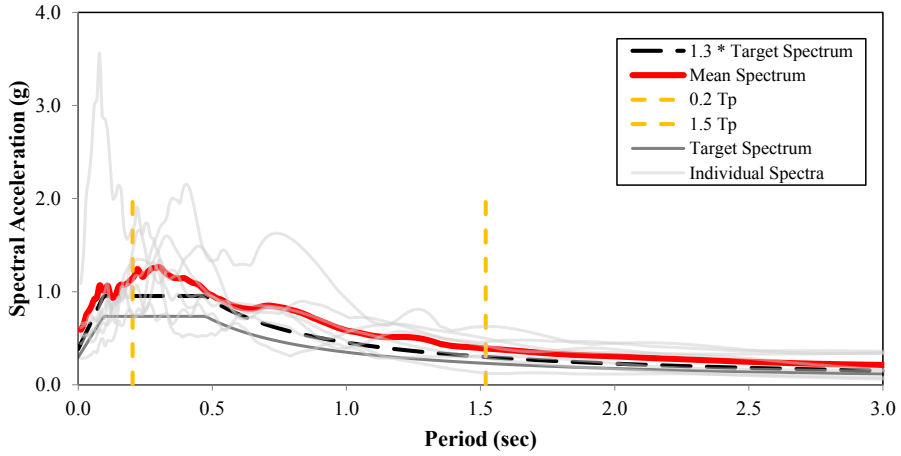

Figure 5: Elastic response spectra for selected ground motions with 5% damping ratio.

3.2 Rotation of ground motion records

It is a general assumption that the ground motion components affect the global axis of the structure in time history analysis. However, in reality, it is not known at which angle the earthquake ground motion components affect a structure. Furthermore, as per Caltrans [14], the ground motion must be applied at a sufficient number of angles to capture the maximum deformation of all critical components. For this reason, in recent years, researchers have carried out several studies on the effect of critical incidence angle on bridge performance [9, 10, 12, 20]. In this study, horizontal ground motion components were rotated by using linear transformation equations. Ground motion components were recalculated using Equation (7) and the new earthquake record components obtained were applied to the bridge global axis as shown in Figure 6. The $a_1(t)$ and $a_2(t)$ specified in Equation (1) are the original horizontal earthquake records that should be applied to the local axes (1) and (2) determined by the angle θ. However, to be used in the analysis, $a_X(t)$ and $a_Y(t)$ which are their equivalents on the glob-

al axes are converted by linear transformation. With this method, analyses were performed by rotating the original components of ground motion from 0° to 180° at 15° intervals. Also, the horizontal component of ground motion which has the highest PGV was affected to the bridge transverse direction. Vertical component of the ground motions was included in each analysis.

$$\begin{Bmatrix} a_X(t) \\ a_Y(t) \end{Bmatrix} = \begin{bmatrix} cos\theta & -sin\theta \\ sin\theta & cos\theta \end{bmatrix} \cdot \begin{Bmatrix} a_1(t) \\ a_2(t) \end{Bmatrix} \tag{7}$$

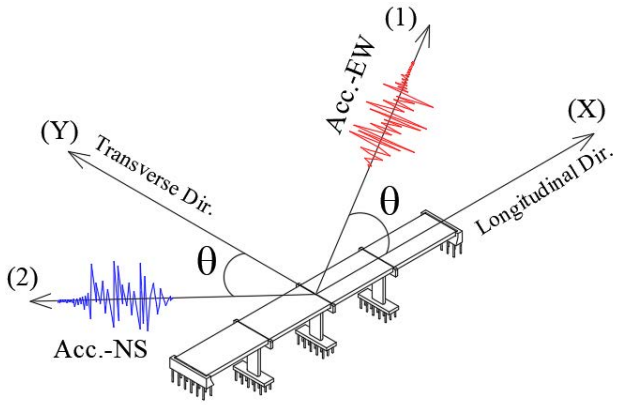

Figure 6: The rotation of the horizontal ground motion pair and its application to the bridge [10]

4 ANALYSIS RESULTS

Nonlinear time history analyses were carried out for given bridge model to investigate the combined effect of scour and earthquake. Scour depth was changed starting from 0 m to 5 m with an increment of 1 m and horizontal ground motion components was rotated from 0° to 180° in counterclockwise direction with an increment of 15°. 6 different scoured bridges exposed to 7 ground motion acceleration time series with 13 particular incidence angles independently. As seen in Figure 7, the 1st and 2nd vibration periods of the bridge increase when scour depth increases. This is because, the clear height of the bent piles increases when the soil around piles is removed. This situation increases the flexibility of the bridge and so do the periods.

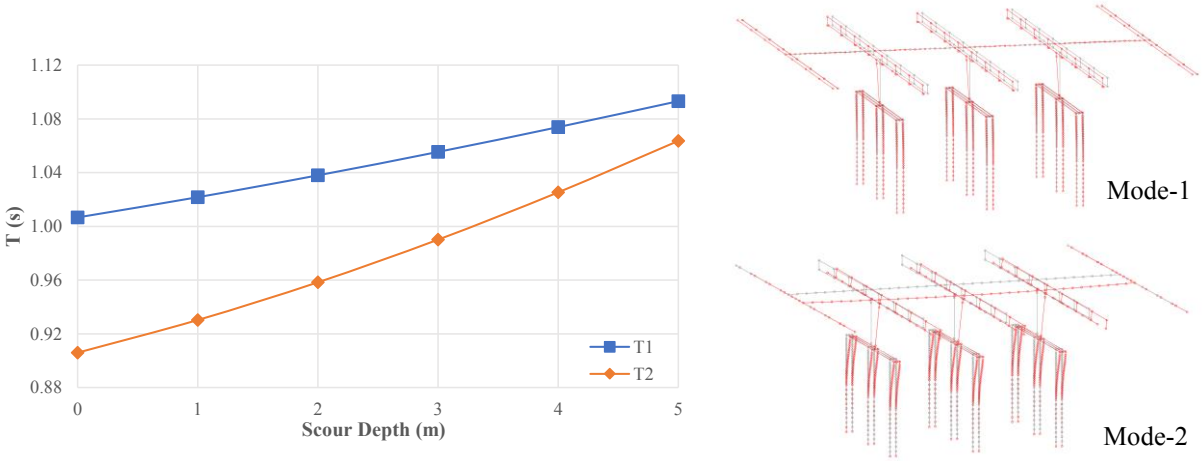

Figure 7: The variation of 1st and 2nd vibration period of bridge depending on uniform scour depth.

Deck displacement in both longitudinal and transverse direction, curvature and shear force demands for bent column piers are inspected as engineering demand parameters and results are given in the sections below.

4.1 Superstructure displacement

Consideration of uniform scour depth change is a practical way while modeling soil structure interaction for the scoured bridges. For each scour depth, nonlinear springs were removed from the pile nodes therefore, the scoured bridge models were obtained easily.

Superstructure displacement demands obtained from nonlinear analysis results belong to the midpoint displacement of the bridge deck. In Figure 8, average maximum displacement demands in longitudinal and transverse direction of the bridge are given. Also, average maximum resultant displacement is calculated by taking the maximum of square root of the sum of squares of these directions. When we examine the results in terms of the change of the earthquake incidence angle, the average maximum displacement in longitudinal direction of bridge has an increasing trend between 0° and 75° although in transverse direction it is decreasing between 0° and 90°. Therefore, the resultant displacement is not much affected from the change of scour depth. According to the radar and bar charts, the average maximum superstructure displacement increases in both directions of bridge when scour depth (H_u) increase uniformly around piles. Because as the depth of scour increases, the effective height of the bridge pier increases, which causes more displacement of the superstructure elements. The maximum difference of average displacement demands in longitudinal direction between no scoured (H_u=0m) and 5 m scoured (H_u=5m) bridge is occurred at 75° incidence angle is 12.4%. In transverse direction, it is at 165° as 18.1%. If it is checked for resultant displacement, the maximum difference becomes 13% at 0° incidence angle.

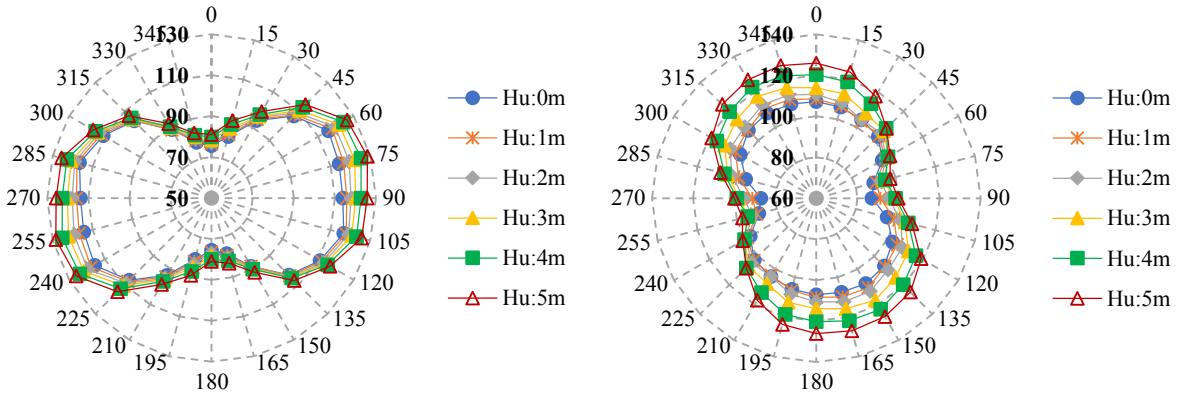

(a) Longitudinal (b) Transverse

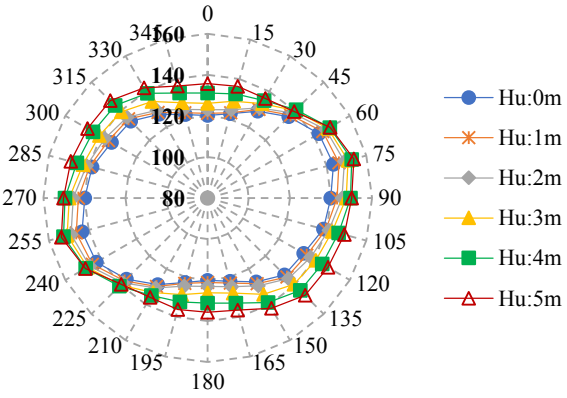
0
15
30
45
60
75
90
105
120
135
150
165
180
195
210
225
240
255
270
285
300
315
330
345
160
140
120
100
80
Hu:0m
Hu:1m
Hu:2m
Hu:3m
Hu:4m
Hu:5m

(c) Resultant

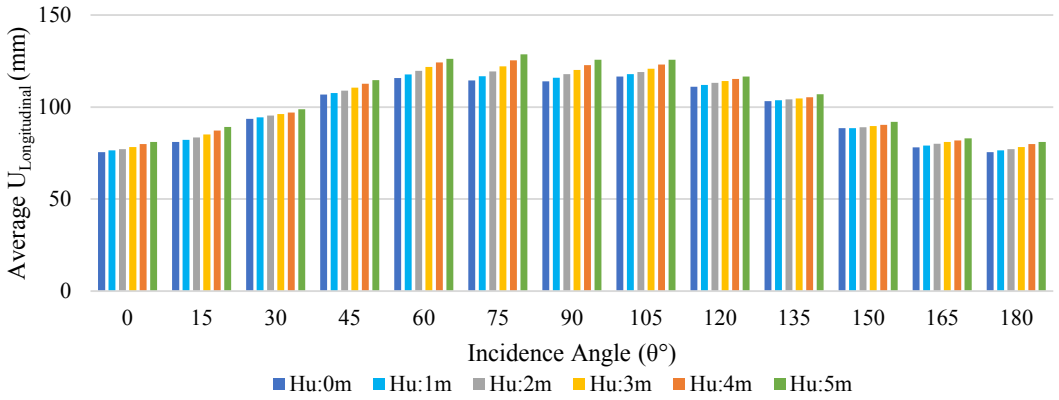
Average U Longitudinal (mm)
150
100
50
0
0
15
30
45
60
75
90
105
120
135
150
165
180
Incidence Angle (θ°)
Hu:0m
Hu:1m
Hu:2m
Hu:3m
Hu:4m
Hu:5m

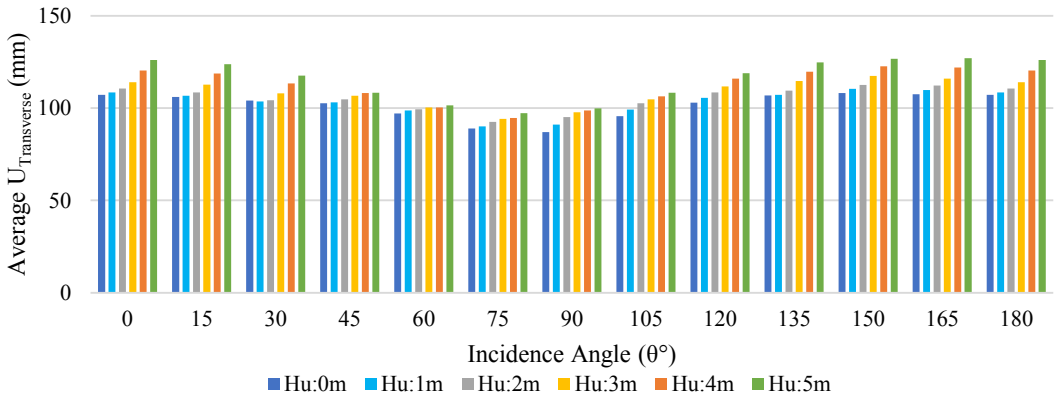
Average U Transverse (mm)
150
100
50
0
0
15
30
45
60
75
90
105
120
135
150
165
180
Incidence Angle (θ°)
Hu:0m
Hu:1m
Hu:2m
Hu:3m
Hu:4m
Hu:5m

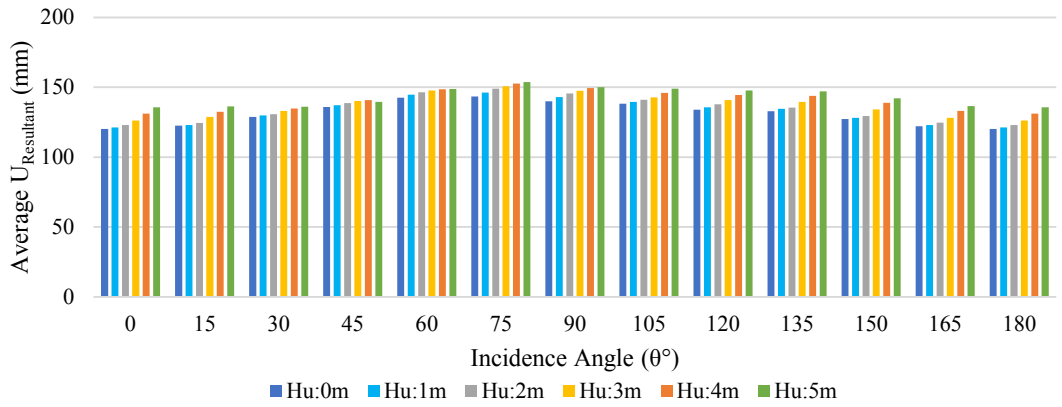

Figure 8: Maximum displacement demands of the bridge for different uniform scour depths and earthquake incidence angles.

4.2 Curvature demand of bridge pier

The superstructure of the bridge maintains in the elastic region due to elastomeric bearings, and these members only transfer axial loads to the bridge columns. Therefore, in terms of nonlinear response during earthquakes, bent columns are the most impacted elements that can expose to seismic damage. Section analyses using the XTRACT program have been carried out for both weak and strong axes to determine the capacity of bridge columns. The yield curvature of the column section is determined by the moment-curvature curves as 0.0033 1/m for the weak axis and 0.0011 1/m for the strong axis.

In Figure 9, the average maximum curvature demands of the middle column of bridge in weak (y') and strong (z') axis is given. Average curvature demand is increasing when ground motion incidence angle is changed from 0° to 75° in weak axis (y'). Also, it is increasing between 0° and 105° in strong axis (z'). Also, average maximum column curvature demand has a decreasing trend when scour depth (H_u) increases in both axes and for all ground motion incidence angles. The reason of this, bridge column becomes more flexible as scour depth increases and this causes to decrease in curvature. Especially in strong axis (z'), the average maximum curvature demand of column is under the yield curvature (Φ_{z_yield}) for all incidence angles when scour depth becomes 4 and 5 m. The maximum difference of curvature demands in the weak axis (y') of column between no scoured (H_u=0m) and 5 m scoured (H_u=5m) bridge is occurred at 0° incidence angle is 45.5%. Also, in strong axis (z'), it becomes 68.7% at 60° incidence angle. These results show that the scour around the piles has a positive contribution to the curvature demands of the bridge column piers.

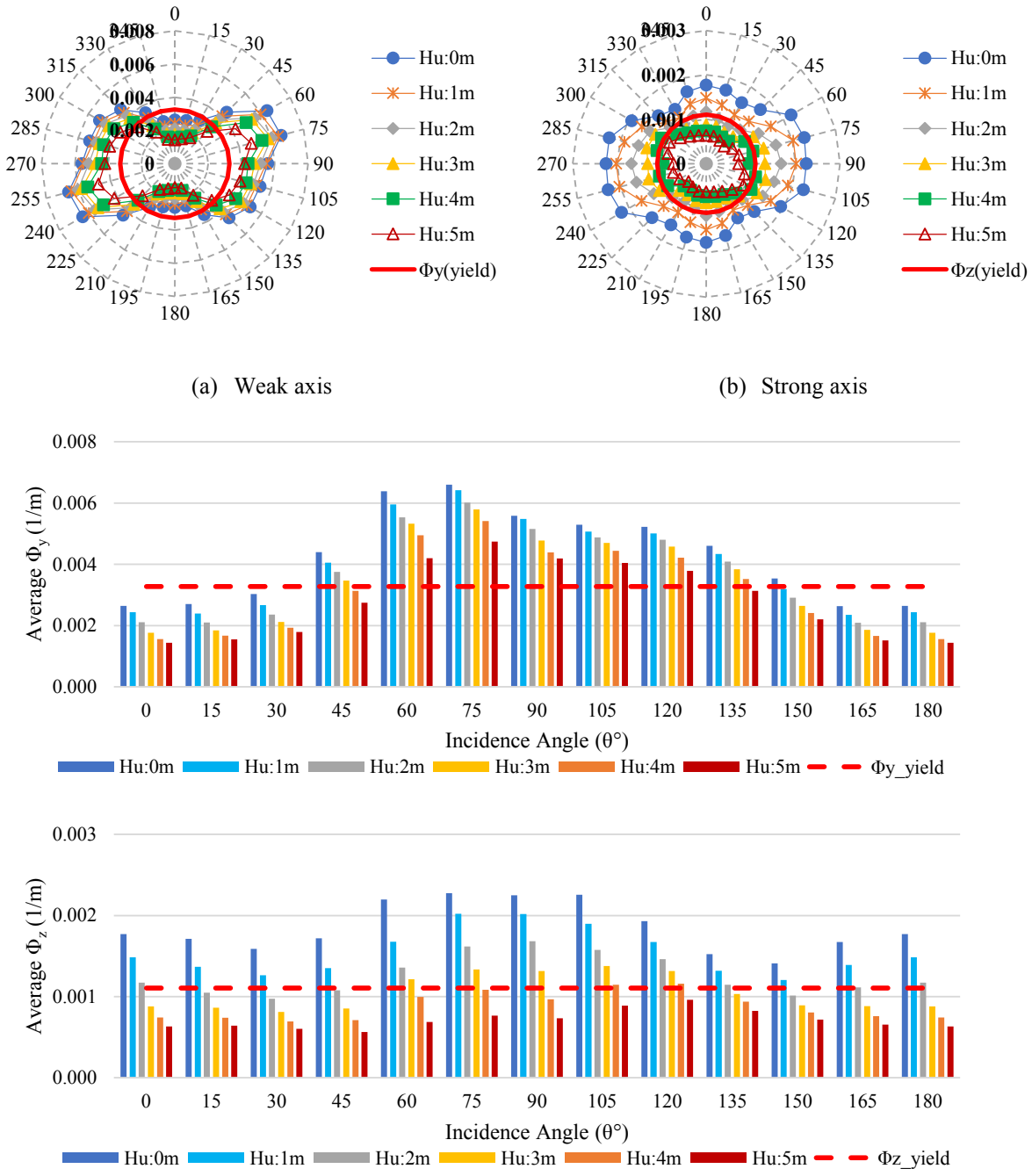

Figure 9: Maximum curvature demands of column weak axis (y') and strong axis (z') for different uniform scour depths and earthquake incidence angles.

4.3 Shear force demand of bridge pier

Member shear force demand, which is a forced-based engineering demand parameter, indicates whether it exceeds its shear capacity. For the purpose of preventing brittle shear failure during earthquakes, all codes recommend ductile section design.

In Figure 10, average maximum shear force demands of the middle column of bridge in local y' and z' axis is given. Average shear demand is decreasing when ground motion incidence angle is changed from 0° to 90° in local y' axis. Besides, it has an increasing trend between that angle range in local z' axis. Moreover, shear force demands decrease as the

depth of scour increases for all incidence angles. The maximum difference of average demands in local y' axis of no scoured (H_u=0m) and 5m scoured (H_u=5m) models occurs at 60° incidence angle and nearly 27.7%. Also, it is about 14.2% at 150° incidence angle in local z' axis. The shear capacity demands of column was calculated in previous sections as 5198.2 kN in local y' axis and 6519.9 kN in local z' axis. When the average maximum shear force demands are compared to these capacities, it is seen that shear force demands are below the limits for all scour depths and incidence angles. Therefore, it can be said that no shear damage occurred in the bridge column during the nonlinear analysis.

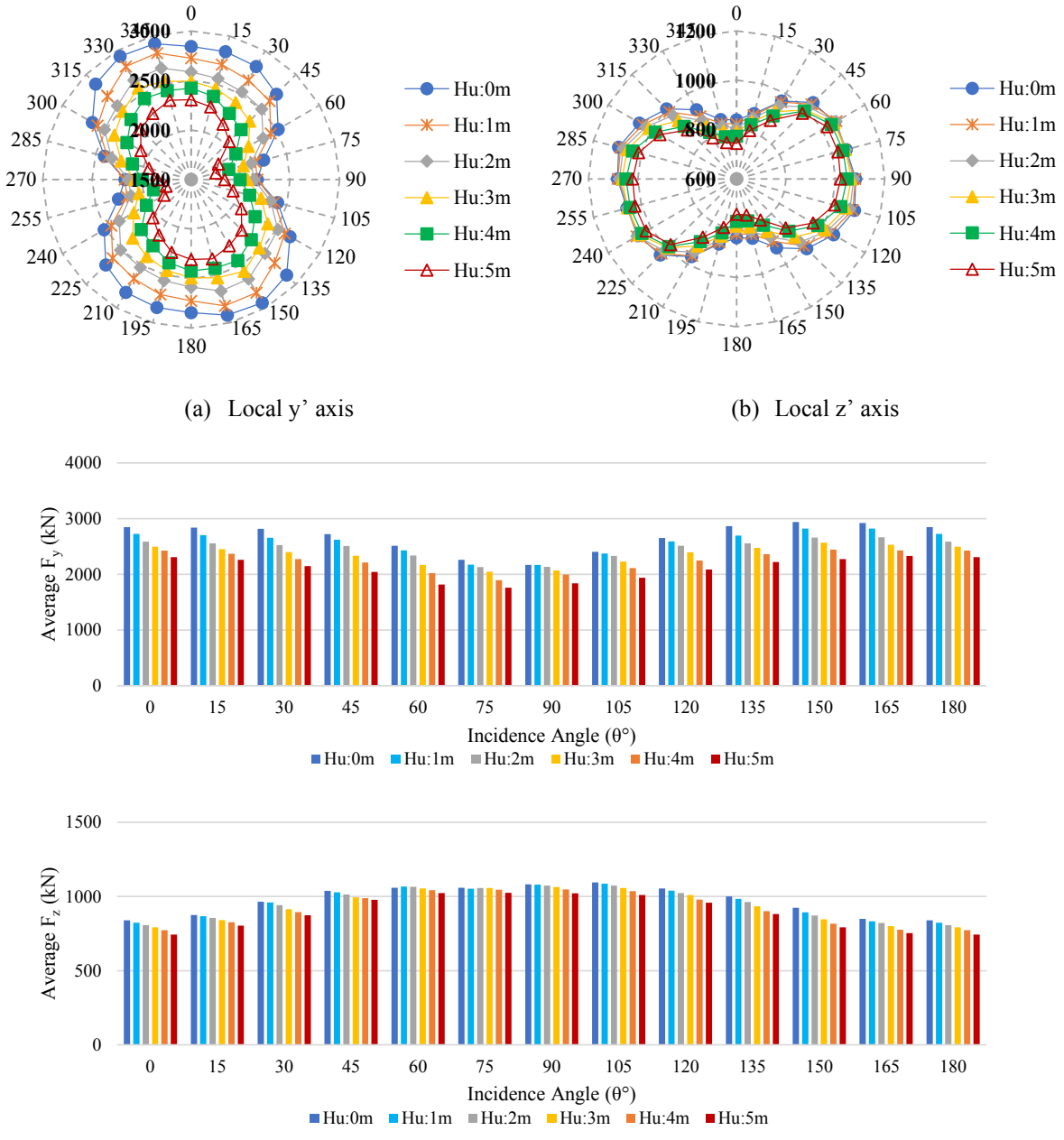

(a) Local y' axis (b) Local z' axis

Figure 10: Maximum shear force demands of column local y' and local z' axis for different uniform scour depths and earthquake incidence angles.

5 CONCLUSIONS

Bridges are one of the critical components of lifeline systems that should be in service during and after a natural disaster. Especially the bridges built on the stream bed, scour may occur over time around substructure members and this situation affects the demand parameters of the bridge elements in the event of an earthquake. Furthermore, ground motion may act on bridges with a different angle and it may cause change in seismic demands. Therefore, a series of nonlinear response history analysis was done for 6 different scoured bridge models by using 7 strong ground motion records with 3 components. Also, horizontal components of ground motions were rotated starting from 0° to 180° with an increment of 15° by using linear transformation equations and demands belong to these bridge models were compared with each other. Below outcomes were achieved from all the investigated parameters;

- Scour is a significant event that has a major impact on the seismic demands of bridge members. Bridge member demands are substantially higher in circumstances of extensive scour than in cases of no scour. Therefore, it is crucial to take it into account when designing bridge-type structures built in flood-prone areas.
- The natural vibration period of the bridge increases with the increase in scour depth. The main cause is an increase in the effective column clear height followed by an increase in scour depth. Therefore, scour increases the vibration periods of the bridge and makes it more flexible.
- Superstructure displacement has an increasing trend with an increase in scour depth for both longitudinal and transverse direction of bridges for all scour cases. Because the effective height of the bridge pier increases along with the depth of scour, as a result superstructure elements displaced more.
- Curvature and shear force demands of bridge column has a decreasing trend with the increase in scour depth. This situation can be explained as the increase in the bridge period results in less earthquake force on the structure. Additionally, in the fixed supported situation, the deformations are primarily concentrated in the bridge columns. However, in scour conditions, the deformations in the piles lessen the deformations in the columns.
- For each demand parameter, there is no particular ground motion incidence angle that results in the most critical seismic demands. It depends on a variety of factors, including the ground motion data used, the chosen soil type, the characteristics of the bridge, the scour depth, etc. However, analytical results demonstrate that it significantly affects demand parameters. Especially superstructure displacement and curvature demand have an increasing trend between 0° and 75° earthquake incidence angles. Therefore, ground motion directionality should be considered in nonlinear time history analysis. According to Caltrans [14], each set of ground motions shall be rotated in 45° increments for at least a total of three angular directions (i.e., 0°, 45°, and 90°) to maximize the structural response. As a result, the analysis of the earthquake incidence angle within the scope of the study highlights the significance of this regulation's article.

REFERENCES

[1] T. Yilmaz and O. C. Aygin, Çoklu Bozulma Etkileri Alt ı nda Ya ş lanan Karayolu Köprülerinin Sismik Kırılganlık ve Riskinin Değerlendirilmesi, no. October, 2019.

[2] Ö. Avsar, B. Atak, and A. Caner, In-Depth Investigation of Seismic Vulnerability of an

Aging River Bridge Exposed to Scour, *J. Perform. Constr. Facil.*, vol. 31, no. 5, pp. 1–13, 2017.
[3] L. G. He, H. H. Hung, C. Y. Chuang, and C. W. Huang, Seismic assessments for scoured bridges with pile foundations, *Eng. Struct.*, vol. 211, no. October 2019, p. 110454, 2020.
[4] F. H. Administration, *Evaluating scour at bridges (HEC-18), fifth edition*, no. 18. 2012.
[5] A. Alipour and B. Shafei, Performance Assessment of Highway Bridges Under Earthquake and Scour Effects, *15th World Conf. Earthq. Eng.*, vol. 18, no. 18, 2012.
[6] X. Guo and Z. Chen, Lifecycle multihazard framework for assessing flood scour and earthquake effects on bridge failure, *ASCE-ASME J. Risk Uncertain. Eng. Syst. Part A Civ. Eng.*, vol. 2, no. 2, pp. 1–10, 2016.
[7] X. Guo, Y. Wu, and Y. Guo, Time-dependent seismic fragility analysis of bridge systems under scour hazard and earthquake loads, *Eng. Struct.*, vol. 121, pp. 52–60, 2016.
[8] I. F. Moschonas and A. J. Kappos, Assessment of concrete bridges subjected to ground motion with an arbitrary angle of incidence: Static and dynamic approach, *Bull. Earthq. Eng.*, vol. 11, no. 2, pp. 581–605, 2013.
[9] A. Roy, G. Bhattacharya, and R. Roy, Maximum credible damage of RC bridge pier under bi-directional seismic excitation for all incidence angles, *Eng. Struct.*, vol. 152, pp. 251–273, 2017.
[10] B. Atak, Ö. Avşar, and A. Yakut, Directional effect of the strong ground motion on the seismic behavior of skewed bridges, *Proc. Int. Conf. Struct. Dyn. , EURODYN*, vol. 2014-Janua, no. June, pp. 1253–1258, 2014.
[11] U. R. Bhatnagar and S. Banerjee, Fragility of skewed bridges under orthogonal seismic ground motions, *Struct. Infrastruct. Eng.*, vol. 11, no. 9, pp. 1113–1130, 2014.
[12] H. R. Noori, M. M. Memarpour, M. Yakhchalian, and S. Soltanieh, Effects of ground motion directionality on seismic behavior of skewed bridges considering SSI, *Soil Dyn. Earthq. Eng.*, vol. 127, no. July, p. 105820, 2019.
[13] Ministry of Transport and Infrastructure of The Republic of Turkey, Principles for the Design of Highway and Railroad Bridges and Viaducts Under the Impact of Earthquakes, 2020.
[14] Caltrans, Seismic Design Criteria, State of California Department of Transportation, no. April, 2019.
[15] S. Banerjee Basu and M. Shinozuka, Effect of ground motion directionality on fragility characteristics of a highway bridge, *Adv. Civ. Eng.*, vol. 2011, 2011.
[16] T. Yilmaz, S. Banerjee, and P. A. Johnson, Performance of Two Real-Life California Bridges under Regional Natural Hazards, *J. Bridg. Eng.*, vol. 21, no. 3, p. 04015063, 2016.
[17] API, Recommended Practice for Planning , Designing and Constructing Fixed Offshore Platforms — Working Stress Design, *Api Recomm. Pract.*, vol. 24-WSD, no. December 2000, p. 242, 2000.
[18] F. H. Kulhawy, Drilled Shaft Foundations, *Found. Eng. Handb.*, vol. 1991, no. c, pp. 537–552, 1991.
[19] R. L. Mosher, Load-Transfer Criteria for Numerical Analysis of Axially Loaded Piles in Sand, 1984.
[20] PEER, PEER Ground Motion Database - PEER Center, https://ngawest2.berkeley.edu/ (accessed Jun. 24, 2021).
[21] TEHM, Turkish Earthquake Hazard Map, https://tdth.afad.gov.tr (accessed Dec. 06, 2021).

[22] Y. Wang, L. Ibarra, and C. Pantelides, Effects of Ground Motion Incidence Angles in a Reinforced Concrete Skewed Bridge Retrofitted with Bucking Restrained Braces, *Struct. Congr. 2017 Bridg. Transp. Struct. - Sel. Pap. from Struct. Congr. 2017*, no. Chopra 2012, pp. 481–493, 2017.